machines

MDPI

Article

Deep Learning-Based Performance Prediction of Electric Submersible Pumps Under Viscous and Gas–Liquid Flow Conditions

Haiwen Zhu [1,*], Hong Yu [2,*], Qiang Sun [1], Qiuchen Wang [1], Haorong Jing [1] and Rakhymzhan Abdikadyrov [1]

[1] McDougall School of Petroleum Engineering, The University of Tulsa, Tulsa, OK 74104, USA; suq5501@utulsa.edu (Q.S.); qiw3387@utulsa.edu (Q.W.); haj2879@utulsa.edu (H.J.); raa7544@utulsa.edu (R.A.)
[2] College of Elementary Medicine, North China University of Science and Technology, Tangshan 063000, China
* Correspondence: haiwen-zhu@utulsa.edu (H.Z.); yuhong@ncst.edu.cn (H.Y.)

Abstract: Electric Submersible Pumps (ESPs) play a pivotal role in the petroleum industry, but their performance is significantly affected by factors such as oil viscosity, gas–liquid ratios, and solid content. Traditional performance prediction methods, including polynomial fitting and mechanistic modeling, often lack adaptability and efficiency, requiring extensive empirical testing. This study leverages experimental data from the viscous and gas–liquid flow tests reported in the literature to benchmark various prediction methods. This research provides a comparative analysis of traditional curve-fitting methods, mechanistic modeling, and seven machine learning approaches. A key innovation of this study is an in-depth sensitivity analysis of different machine learning methods, especially focused on neural network parameters, such as activation functions and training configurations, to assess their impact on prediction accuracy and identify optimal network designs. Furthermore, a pump testing methodology is introduced to significantly reduce testing costs while maintaining a high prediction accuracy. The findings demonstrate the advantages of machine learning over traditional methods, including an enhanced prediction accuracy, practical guidelines for efficient parameter tuning, and the ability to address incomplete pump curve data. These contributions not only highlight the value of integrating machine learning into ESP modeling and operational workflows but also pave the way for future advancements in universal modeling frameworks for diverse ESP applications.

Keywords: electric submersible pump; deep learning; convolutional neural network; multiphase flow; artificial lift

check for updates

Academic Editors: Davide Astolfi and Jong-Myon Kim

Received: 11 November 2024
Revised: 20 January 2025
Accepted: 23 January 2025
Published: 10 February 2025

Citation: Zhu, H.; Yu, H.; Sun, Q.; Wang, Q.; Jing, H.; Abdikadyrov, R. Deep Learning-Based Performance Prediction of Electric Submersible Pumps Under Viscous and Gas–Liquid Flow Conditions. *Machines* **2025**, *13*, 135. https://doi.org/10.3390/machines13020135

Copyright: © 2025 by the authors. Licensee MDPI, Basel, Switzerland. This article is an open access article distributed under the terms and conditions of the Creative Commons Attribution (CC BY) license (https://creativecommons.org/licenses/by/4.0/).

1. Introduction

Electric Submersible Pumps (ESPs) are one of the most used artificial lift methods in the oil and gas industry. They operate efficiently in various production environments but are highly sensitive to a wide range of factors, such as fluid viscosity, gas content, and solid particles. These variations can significantly impact the performance and longevity of ESPs, making performance prediction a crucial task for ensuring their optimal operation and reducing downtime. Traditional methods of ESP performance prediction rely heavily on empirical data and polynomial fitting, requiring extensive testing under different conditions. While these methods have been widely adopted in the industry, they are time-consuming, resource-intensive, and prone to inaccuracies when faced with dynamic flow conditions. Another approach is mechanistic modeling, which utilizes physical principles to predict

pump behavior. However, these models can be complex and difficult to adapt to field-specific variations [1–5].

In recent years, the application of machine learning techniques, particularly deep learning, has gained significant attention for solving complex prediction problems. Most of the recent advancements in machine learning (ML) on ESP focuses on failure detection and well surveillance [5–10]. Studies have demonstrated the application of ML algorithms, such as deep learning and random forests, for anomaly detection and failure prediction, enabling proactive maintenance and minimizing downtime. Techniques like autoencoders and digital twins integrated with ML models have been utilized for real-time monitoring and failure prediction, achieving notable accuracy in detecting operational anomalies.

Conversely, the application of deep learning architectures in pump performance prediction requires diverse machine learning models tailored to specific tasks. Han et al. (2019), Dutta et al. (2018), and Mohammadzaheri et al. (2020) have explored how deep learning techniques, particularly convolutional neural networks (NNs), can be leveraged to model complex flow patterns and pump behaviors [11–13]. These studies emphasize that traditional empirical and mechanistic models, while effective in many cases, often struggle to account for the intricate relationships between multiple influencing factors such as gas–liquid ratios, viscosity, and pump geometry. Deep learning offers a data-driven approach that can capture these non-linearities, improving the accuracy of performance predictions.

Han et al. (2019) explored a method for predicting the performance of centrifugal pumps using a double hidden layer backpropagation (BP) neural network combined with the Levenberg–Marquardt (LM) algorithm [11]. Their results show that this method improves the accuracy and convergence speed compared to traditional single hidden layer models [11]. Similarly, Dutta et al. (2018) focused on integrating deep learning with ESP design, using neural networks to predict the impact of changes in pump geometry on overall system performance [12]. These findings suggest that deep learning can play a pivotal role in enhancing ESP design processes, particularly in optimizing stage geometry and flow passage dimensions to maximize efficiency.

Other challenges in ESP systems are optimizing performance under varying operating conditions and fault detection. Mohammadzaheri et al. (2016) and Syed et al. (2022) contributed to the growing body of research on ESP system optimization [14,15]. Their studies focused on the use of deep learning to optimize ESP operations, proposing neural networks that can dynamically adjust pump parameters in real time, based on changing production conditions. This adaptability, coupled with the ability to process large datasets from field operations, allows for a more proactive approach to managing ESP systems, reducing downtime and increasing overall operational efficiency. The authors also highlight the potential for deep learning to assist in predictive maintenance, identifying patterns in pump behavior that precede failures or efficiency drops. Kumar et al. (2020), Orru et al. (2020), and Guo et al. (2015) explored the application of neural networks for detecting anomalies in ESP operation [16–18]. These studies suggest that NNs and other deep learning architectures can be trained to recognize the early warning signs of mechanical failures, such as changes in vibration patterns, temperature fluctuations, or pressure irregularities. By identifying faults early, operators can take corrective action before catastrophic failures occur, thereby extending the life of the equipment and reducing maintenance costs.

In ESP performance prediction, traditional methods such as polynomial fitting and advanced mechanistic modeling [1,19,20] have inherent limitations, and there remains a significant gap in understanding how to effectively tune and select appropriate machine learning methods for ESP performance prediction. Therefore, this study reviewed and compared the predictions of different machine learning methods, including Generalized Additive Models (GAMs), Support Vector Regression (SVR), Gaussian Process Regression

(GPR), Radial Basis Function (RBF), Gradient-Boosting Machines (GBMs-XGboost), Kernel Ridge Regression (KRR), and Fully Connected Neural Networks (FNNs) [21–27]. All seven methods are summarized in Table 1 and can be used to investigate the non-linear relationship between pump performance and fluid properties, i.e., viscosity and gas void fractions. Additionally, a comprehensive comparison was conducted among polynomial fitting, mechanistic modeling, and machine learning. While advanced AutoML techniques like Optuna were incorporated, we addressed their limitations in handling incomplete pump curve data and computational cost challenges. By narrowing the parameter selection ranges, our work improved their efficiency, reducing the reliance on trial-and-error approaches. This study also underscores the potential of integrating advanced machine learning techniques into ESP performance prediction workflows, contributing to reduced testing costs and inspiring further research into universal neural network models for diverse flow conditions.

Table 1. Summary of different machine learning method.

Method	Advantages	Disadvantages
GAM	Interpretable, flexible, smooth, non-linear relationships.	Less effective when iterations between variables are significant.
SVR	Effective for small, non-linear datasets.	Expensive for large datasets; lacks probabilistic outputs.
GPR	Provides probabilistic prediction; preferred for model uncertainty.	Expensive for large datasets.
RBF	Can capture localized, non-linear variations.	Requires careful tuning; avoid overfitting.
GBM-XGboost	For large datasets, non-linear relationships, and feature importance analyses.	Less interpretable; no inherent probabilistic output.
KRR	Captures non-linear relationships effectively.	Expensive for large datasets; less intuitive than GBM or NN.
FNN	Handles complex, non-linear relationships.	Requires more data for training; sensitive to parameters.

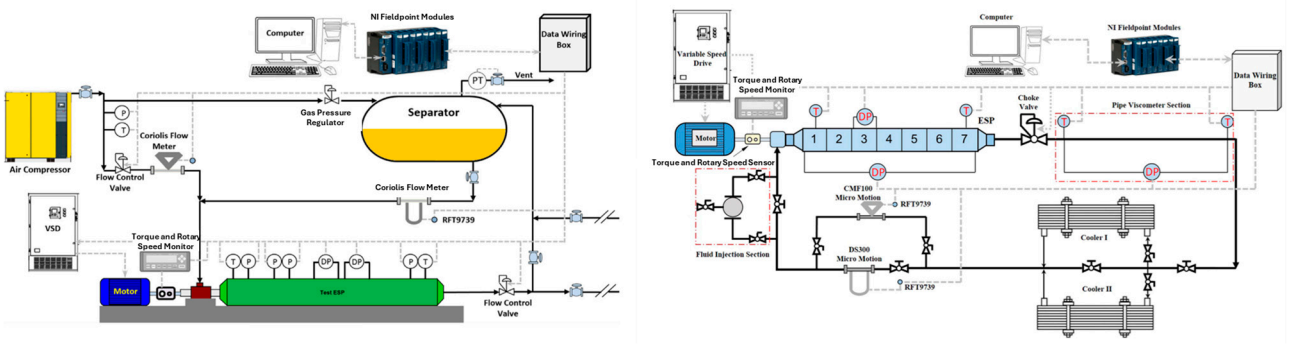
2. Materials and Methods

The data used in this study were collected through an extensive series of tests conducted by the TUALP (The University of Tulsa Artificial Lift Project) on ESPs. Historically, ESP performance data have been analyzed using traditional curve-fitting methods, and mechanistic models were developed. In this study, a deep learning approach, specifically a neural network (NN), was developed to predict ESP performance. The details of the data collection and methodology are illustrated in this section.

2.1. Experimental Setup and Data Collection

This study utilized data from experimental tests on Electric Submersible Pumps (ESPs) under different operating conditions, including viscous fluid flow and gas–liquid mixtures. The tests were conducted using a specialized ESP testing facility as shown in Figure 1, designed to simulate field conditions and capture pump performance metrics. The collected data include, but are not limited to, the flow rate (both liquid and gas phases), pump pressure differentials across the stages, viscosity of the working fluid, pump speed (RPM), power consumption (horsepower), and gas–liquid ratio. The data collection was performed under a range of operating conditions to capture the sensitivity of the ESP performance to changes in the fluid viscosity and the gas content. The experimental setup was calibrated before each test to ensure the accuracy and the repeatability of the measurements. The

experimental results are available in our previous publications [19–21]. All the tests were conducted in accordance with the industry testing standards. For the high-viscosity tests, the oil temperature was controlled using a heat exchanger, and at least 60 data points were collected for each flow condition within a specified temperature range. For the gas–liquid tests, two testing procedures were employed. The first followed a similar approach to the high-viscosity tests, collecting at least 60 data points for each flow condition. The second involved continuous testing, where either the gas or the liquid flow rate was held constant while the other was gradually varied. Each curve was repeated at least three times to ensure the reliability and the consistency of the results.



(**a**) (**b**)

Figure 1. Experimental facility setup. (**a**) ESP gas–liquid flow loop [1]; (**b**) ESP high-viscosity flow loop [21].

This study utilized pump curves from our previous work [1,19,20] to train the neural network (NN) model and compare it to traditional fitting methods and mechanistic models. The ESP gas–liquid performance curves were sourced from the GC6100 tests [1], while the high-viscosity flow curves were derived from ESP3 and MTESP (a pseudonym used due to confidentiality agreements). The original MTESP viscosity test was conducted with low-to-mid-viscosity oil (400 cP). To extend the dataset, Computational Fluid Dynamics (CFDs) simulations were used to generate MTESP pump curves up to 1500 cP, as the NN model can be trained with both experimental and simulated data.

2.2. Polynomial Fitting and Interpolation

As a baseline for the comparison, polynomial fitting and interpolation were used to predict the ESP performance based on the collected experimental data. This method involved fitting a polynomial function to the performance curves generated by the test data. The degree of the polynomial was selected based on minimizing the error between the predicted and the actual performance, i.e., avoiding an unphysical fitted curve, like being tail-up under high-flow-rate conditions.

The default polynomial degree for the water curve is typically set to 5. However, this can lead to overfitting in regions of low or high flow rates because most pump curve tests focus primarily on the pump's working range (e.g., 20–120% of the best efficient point), often neglecting data points at zero flow or zero head (where the flow rate is 0 or the pump head is zero). To address this, it is recommended to use a 2nd- or 3rd-degree polynomial for a single-phase flow unless additional "fake" points are manually created to control the curve shape. Conversely, accurately predicting the pump surging transition (a sudden drop in the pump head) in the ESP gas–liquid flow using polynomial fitting is highly challenging. In this study, an 8th-degree polynomial was applied to the gas–liquid flow tests in Section 3, which captured the general trend but still resulted in significant errors in the surging transition zone.

2.3. Mechanistic Modeling

A mechanistic model, based on the principles of fluid dynamics and ESP design, was implemented for the performance prediction. The TUALP mechanistic model (MTESP) was used to predict pump performance under both viscous and gas–liquid flow conditions. The model incorporated key parameters such as pump geometry, fluid properties, and operational conditions. The results of the mechanistic model served as a second baseline for comparing the effectiveness of the deep learning approach. The model was developed and published in our previous study [19–22].

2.4. Machine Learning Method

In this study, 7 machine learning methods were systematically evaluated to capture the non-linear relationships between the input parameters (e.g., the flow rate, viscosity, and gas–liquid ratio) and the pump's output performance (e.g., the pressure differential). The model was trained using the Adam optimizer, which balances computational efficiency and performance. The dataset was split into training (80%) and validation (20%) subsets. The best structure of each method was automatically tuned by the Optuna framework, and the parameter range is listed in Table 2. By default, 50 Optuna iterations are used in most machine learning methods, while 100 are used for XGboost and 200 are used for NNs due to their complexity. Each method was assessed based on its ability to handle the complex non-linearities and smoothness required for accurate ESP performance predictions.

Table 2. Machine learning methods' design parameters.

Method	Parameter Range
GAM	"lambda 1": 1×10^{-3}–1×10^{3}, "lambda 2": 1×10^{-3}–1×10^{3}
SVR	"C": 0.1–10, "epsilon": 0.01–1, "kernel": ["linear", "rbf", "poly"]
GPR	"kernel": ["RBF", "Matern"], "length scale": 0.1–10, "constant value": 0.1–10
RBF	"number of RBF units": 5–50, "learning rate": 1×10^{-4}–1×10^{-2}, "epochs": 50, 200
GBM-XGboost	"n estimators": 50–1000, "max depth": 1–10, "learning rate": 1×10^{-4}–0.3, "subsample": 0.5–1, "col of sample by tree": 0.5–1, "gamma": 0–10, "reg alpha": 0–10, "reg lambda": 0–10
KRR	"kernel": ["linear", "rbf", "poly", "sigmoid"], "alpha": 1×10^{-3}–1, "gamma": 1×10^{-3}–1
FNN	"layers": 1–3, "neurons": [16, 32, 64, 128], "learning rate": 1×10^{-4}–1×10^{-2}, "batch size": 16, 32, 64, 128, "dropout rate": 0–0.5, "optimizer": ['Adam', 'RMSprop', 'SGD'], "activation function": ['relu', 'sigmoid', 'softmax', 'softplus', 'softsign', 'tanh', 'selu', 'elu', 'exponential']

Among these, NNs outperformed the alternatives, demonstrating their versatility in capturing complex relationships and achieving a high prediction accuracy. The NNs' ability to learn from large datasets and adapt to non-linear patterns made them the most suitable approach for this application. The model's design and training details, as well as its comparative advantage, are illustrated in Figure 2.

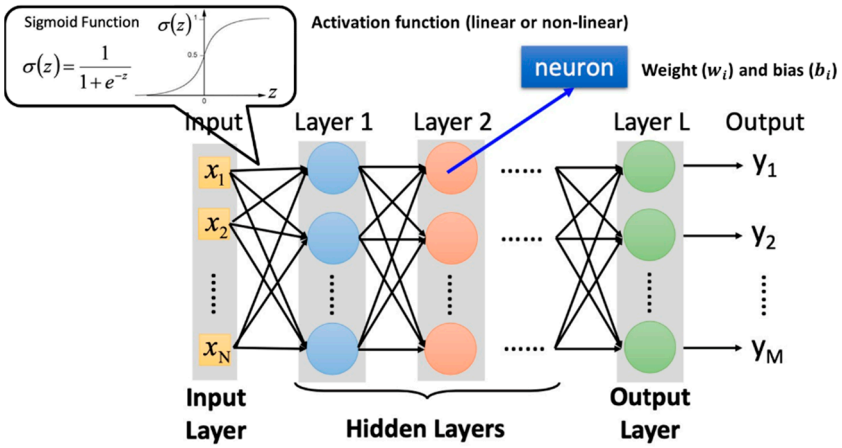


Figure 2. Neural network structure.

2.5. Fully Connected Neural Network (FNN) Sensitivity Studies

A simple FNN structure optimization study was first conducted using the Optuna framework, as shown in Table 2. To further investigate the effectiveness of the activation functions and the training size, a detailed sensitivity analysis was conducted separately, only searching for NN structure parameters including layers, neurons, learning rate, batch size, and dropout rate. The following aspects were investigated:

1. FNN structure: variations in the number of layers, convolutional filters, and kernel sizes were explored to identify the most effective architecture for ESP performance prediction.
2. Activation functions: different activation functions (ReLU, Sigmoid, and exponential) were tested to assess their impact on the model's ability to predict both viscous and gas–liquid flow conditions.
3. Training inputs: The FNN model for gas–liquid pump performance was first trained only by measured data (liquid flow rate, gas flow rate, rotational speed, and head). Then, the calculated data, i.e., the gas void fraction, mixture density, and mixture viscosity, were included for a further investigation into their effectiveness in FNN methods.
4. Testing dataset sensitivity analysis (ESP gas–liquid flow): The original dataset was split into different training and testing sets. The training set was further subdivided into training (80%) and validation (20%) subsets for the general NN model training purpose, while the testing set was used exclusively to evaluate the trained NN model. This study aimed to analyze the effects of the gas flow rate and the rotational speed on the ESP performance. The goal was to determine the optimal testing matrix by balancing prediction accuracy with a reduced test matrix size, thereby significantly lowering the workload and testing costs.

2.6. Comparative Analysis

The results of the FNN predictions were compared with those obtained from polynomial fitting, mechanistic modeling methods, and other machine learning models. Performance metrics, including the mean absolute error (MAE) and the Root Mean Squared Error (RMSE), were calculated to evaluate the accuracy of each prediction method. Additionally, the generalization capabilities of the FNN were tested by predicting the ESP performance beyond the range of the trained data, and the results were analyzed to determine the model's robustness.

3. Results and Discussion

The process reported in this section began by examining the overtraining issue in the NN model, where excessive training led to unphysical pump curves, mitigated through early stopping. The effects of different activation functions were then evaluated, showing how their selection influenced the prediction accuracy. Later, a testing dataset sensitivity analysis was conducted on the ESP gas–liquid flow, aiming to determine the optimal testing matrix for balancing the prediction accuracy and reducing the testing costs by analyzing the gas flow rate and the rotational speed effects. Lastly, the NN model was subsequently compared with polynomial fitting and mechanistic modeling, demonstrating its superior performance, particularly for complex flow conditions.

3.1. Polynomial Fitting and Mechanistic Modeling

This section compares polynomial fitting and interpolation, mechanistic modeling, and different machine learning methods in ESP performance prediction. Firstly, the performance of the ESP was evaluated using polynomial fitting for both viscosity and gas–liquid flow tests, as shown in Figure 3. The viscosity test fitting with a polynomial degree of three (n = 3) provided reasonably accurate results, with the fitted curves closely matching the experimental data across a range of viscosities (from 1 cP to 1500 cP). To further evaluate the polynomial fitting approach, interpolation was used to predict the ESP performance for intermediate viscosities and gas flow rates that were not directly measured. For instance, in the viscosity test, fitted curves for 1, 50, and 200 cP were used to interpolate the performances for 10 and 100 cP. As shown in the figures, the results of the interpolation were mostly acceptable, with only minor deviations between the interpolated and the actual experimental data. This indicates that the polynomial fitting and interpolation method is generally suitable for modeling viscosity impacts on ESP heads. However, it should be noted that high-quality test and simulation data were used in this study. It was also common that tests were only conducted for the working range (around the pump best efficiency point). As a result, the fitting method may have suffered from an unphysical head and tail shape, e.g., a tail-up curve.

In the case of the gas–liquid flow (mapping test with n = 8), polynomial fitting showed significant limitations, especially near the surging points. These surging points, characterized by sudden changes in the performance curve, were not captured effectively, resulting in poor fitting and inaccuracies at critical regions. In addition, interpolation in the ESP gas–liquid flow led to significant inaccuracies, particularly in regions where the flow conditions rapidly changed, such as the surging area. The inability of polynomial fitting to accurately model these complex dynamics points to the limitations of this approach for gas–liquid systems, where highly non-linear behavior is common.

Mechanistic modeling, unlike data-driven or fitting–interpolation methods, does not require training data to predict the pump performance under different flow conditions. Instead, it relies on physical equations and pump-specific parameters. As shown in Figure 4, the mechanistic model accurately predicted the ESP performance under both high-viscosity and gas–liquid flow conditions. The predicted curves closely match the experimental data, showcasing the effectiveness of this approach under controlled conditions. However, the application of mechanistic modeling is limited by the need for detailed pump geometry information, which is often confidential and not easily accessible. This poses a significant challenge for widespread adoption, as the geometry details are crucial for making accurate predictions but may be proprietary or difficult to obtain from manufacturers. Additionally, the range of the applicability of mechanistic models remains an issue. For instance, when the gas concentration is too high, the model struggles to accurately predict surging boundaries, which limits its ability to represent highly complex multiphase flows.

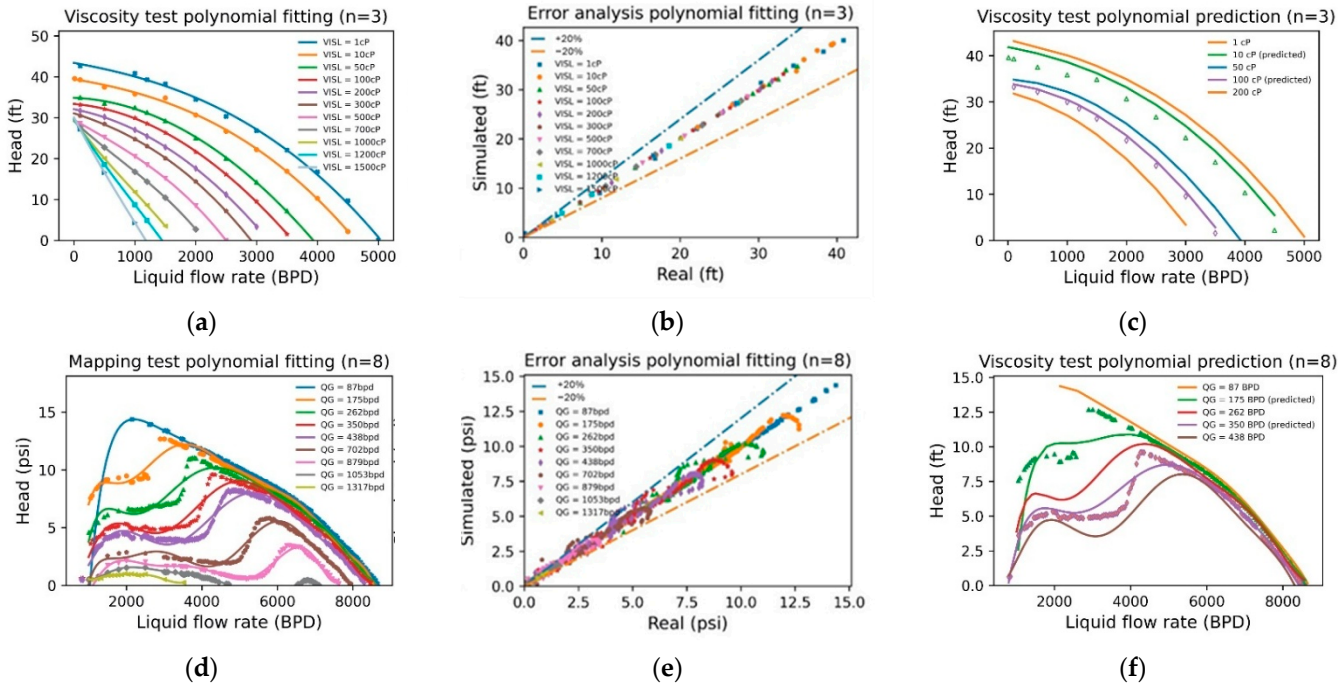


Figure 3. Polynomial fitting and interpolation for ESP high-viscosity flow and gas–liquid flow. (**a**) MTESP viscous flow fitting result. (**b**) MTESP viscous flow fitting error. (**c**) MTESP viscous flow interpolation. (**d**) GC6100 gas–liquid fitting result. (**e**) GC6100 gas–liquid fitting error. (**f**) GC6100 gas–liquid interpolation.

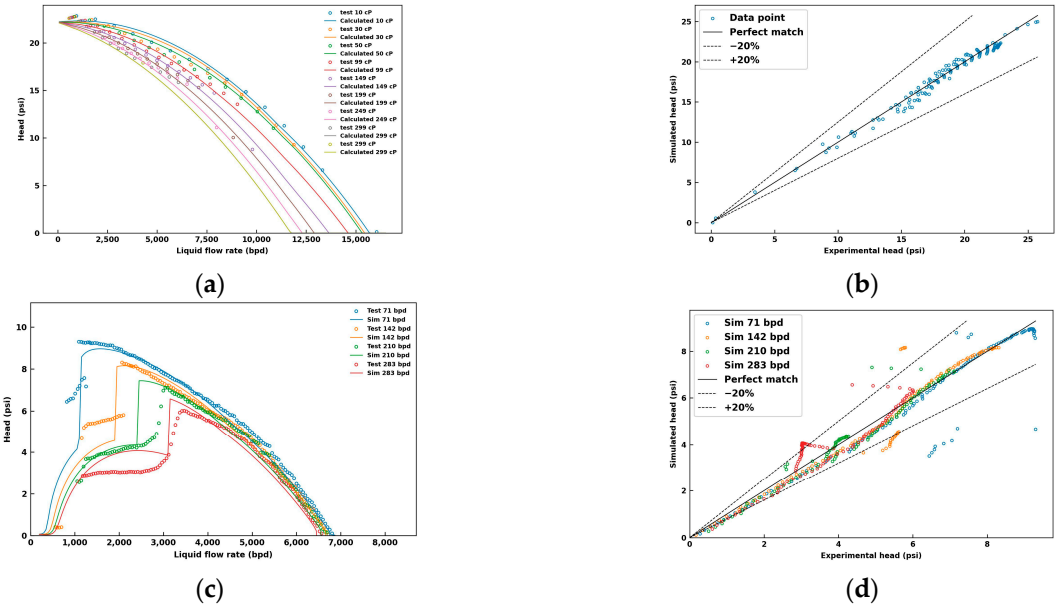


Figure 4. Mechanistic model [1,19] for ESP high-viscosity flow and gas–liquid flow. (**a**) MTESP viscous flow mechanistic model result. (**b**) MTESP viscous flow mechanistic model error. (**c**) GC6100 gas–liquid flow mechanistic model result at 2400 RPM. (**d**) GC6100 gas–liquid flow mechanistic model error at 2400 RPM.

In summary, while polynomial fitting with interpolation provides a quick and easy method for estimating ESP performance under steady conditions such as viscosity variations, its application to more dynamic conditions, such as gas–liquid flows, is limited. The poor performance in capturing surging points and abrupt changes highlights the need for more advanced predictive models capable of addressing the non-linearities inherent in

multiphase flow dynamics. On the other hand, mechanistic modeling predicted the ESP performance accurately under many conditions. However, its reliance on detailed pump geometry and its limited performance at high gas concentrations underscore the need for complementary methods, such as deep learning, which can overcome these limitations through data-driven adaptability.

3.2. Comparison Among Different Machine Learning Methods

All of the machine learning models were initially trained using a relatively small dataset, specifically the ESP3 high-viscosity flow pump curve dataset. The optimal model structures were determined using the Optuna framework. Figure 5 presents the final model structures, the mean square error (MSE), and the predictions, with the figure titles highlighting the model structures and corresponding loss information. The results indicate that the GAM, RBF, and XGBoost models failed to accurately predict the pump performance. While the SVR and KRR models exhibited low MSE values, their predictions did not align with the physical shape of the pump performance curve, particularly in the tail region. In contrast, only the GPR and FNN models produced predictions that both accurately captured the pump performance and adhered to the physical pump curve shape.

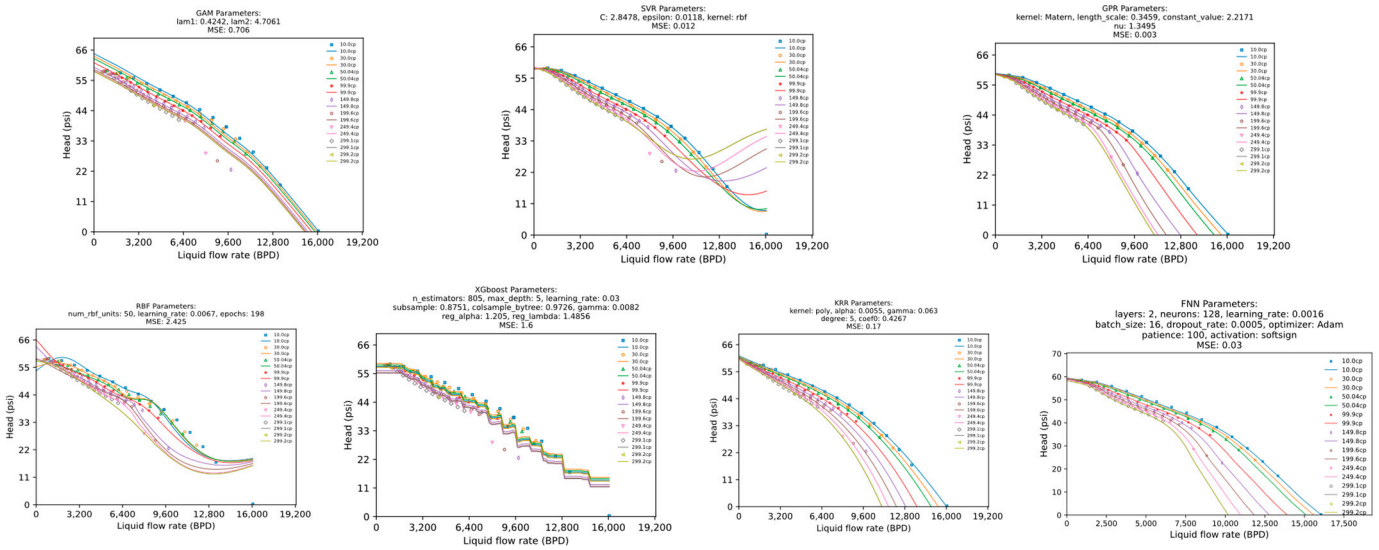


Figure 5. Machine learning model structures and predictions (ESP 3 high-viscosity tests).

To further evaluate the performance of different models, GPR, KRR, and FNN were selected and trained using the MTESP high-viscosity dataset (CFD study), which includes more data points in the high-flow-rate region to potentially reduce prediction uncertainty. The three models were also trained on the GC6100 gas–liquid curves dataset to assess their performance in a more complex pump fluid flow scenario. As shown in Figure 6, all three models achieved a low mean square error (MSE) in their pump performance predictions. However, the GPR model exhibited a noticeable "jumping" trend when applied to the MTESP viscosity dataset, and both the GPR model and the KRR model provided unreliable predictions at certain flow rates in the ESP gas–liquid flow. Furthermore, the GPR model required significantly more training time due to the larger dataset and the complexity of its modeling approach.

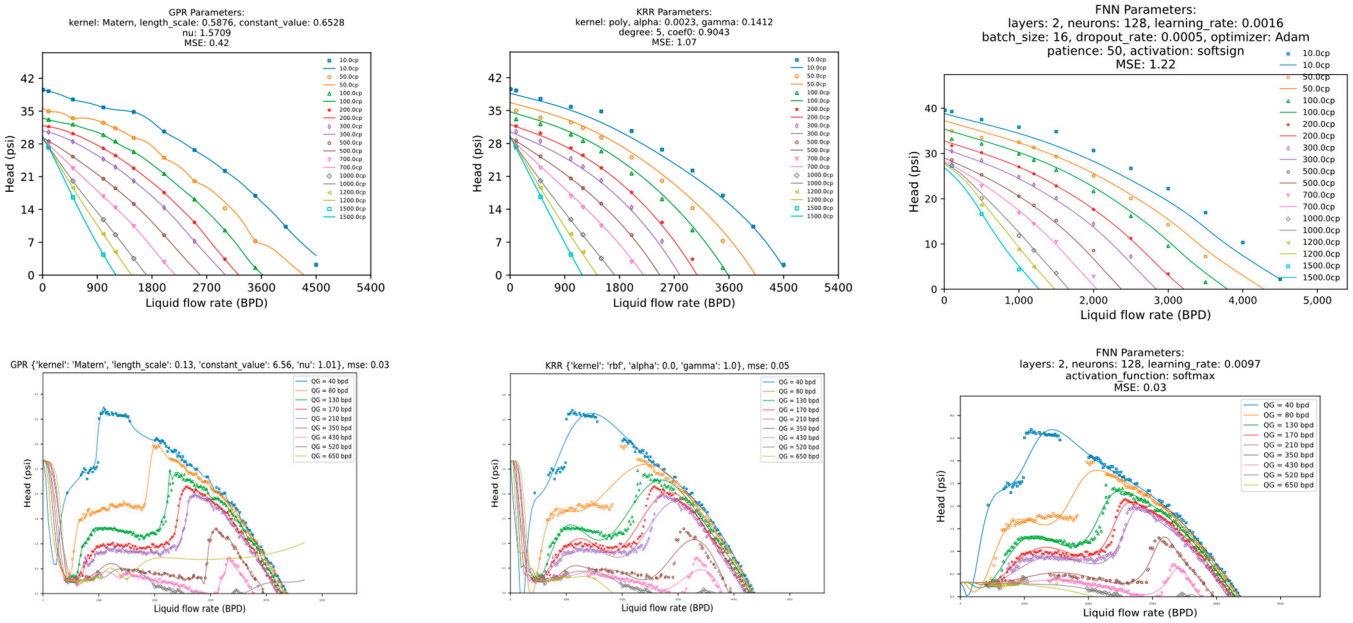


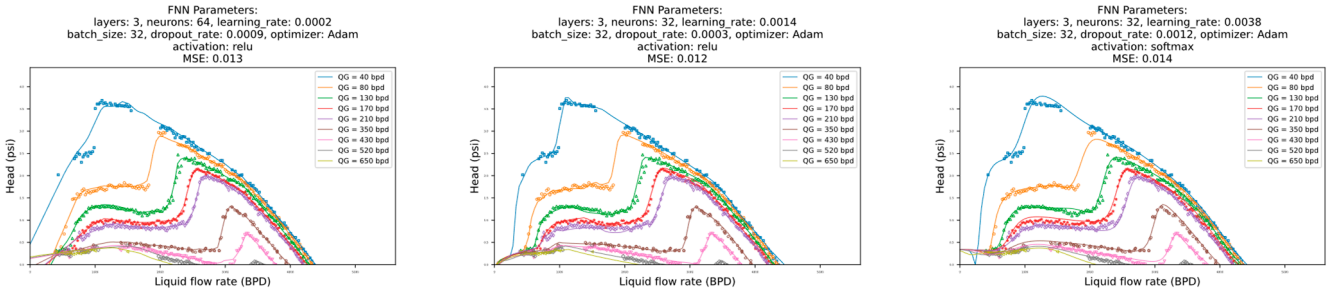
Figure 6. Machine learning model structures and predictions (MTESP high-viscosity test and GC6100 gas–liquid test).

In summary, the FNN model demonstrated greater flexibility and reliability in predicting the ESP performance, particularly given the challenges of obtaining data points at extreme high and low flow rates due to excessive friction losses and gas lock issues. In the absence of a complete pump curve, the GPR and KRR models may produce unphysical predictions, whereas the FNN model allows for better control over the shape of the predicted pump curve by selecting appropriate activation functions. Detailed analyses are provided in the following section.

3.3. Training Input Parameters

The ESP performance test datasets focused on isolating the effects of individual fluid properties by varying only one parameter at a time, such as the gas volumetric flow rate or the liquid viscosity. This approach allowed for a detailed analysis of each property's impact. As demonstrated in the ESP viscosity performance tests, when sufficient data were available, the predicted pump curve was very smooth, and the FNN models effectively revealed the relationship between the pump performance and the liquid viscosity. However, when directly using the measured gas–liquid test data—such as liquid flow rate, gas flow rate, head, and speed—to train the FNN model, its performance was less reliable at the surging point, where the pump performance suddenly dropped at low liquid flow rates. To address this limitation, calculated parameters are being explored to improve and innovate the neural network algorithm.

Figure 7a illustrates the FNN predictions trained solely on the original measured data points, including the liquid flow rate, gas flow rate, head, and speed. The results show that this approach failed to capture the two-step changes in the pump surging performance. In contrast, Figure 7b,c depict the predictions obtained after adding calculated parameters, such as the pump intake gas void fraction (GVF), mixture fluid density, and mixture fluid viscosity. Although these parameters are straightforward calculations derived from gas and liquid flow rates, the inclusion of the GVF clearly improved the prediction accuracy of the FNN model.



(**a**) (**b**) (**c**)

Figure 7. FNN model with different training inputs (GC6100 gas–liquid tests): (**a**) only original data; (**b**) original data and GVF; and (**c**) original data, GVF, mixture density, and mixture viscosity.

However, it is also evident that adding more training parameters increases the complexity of the problem and can lead to unstable predictions, particularly where the testing points are sparse. For instance, as shown in Figure 7c, the inclusion of additional parameters may even reduce the model's accuracy. Based on these findings, it is recommended to calculate and include only GVF as a training parameter for the FNN model when applied to ESP gas–liquid flow predictions.

3.4. Activation Function Analysis

In this study, nine activation functions (as shown in Figure 8) were compared and evaluated for predicting ESP performance under gas–liquid and high-viscosity flow conditions. Each activation function has a unique shape, which influences how well it can model the physical trends of the data. Selecting the optimal activation function is crucial to accurately capturing the performance curves while avoiding unphysical results, particularly at the head and tail of the predicted ESP performance curves under different flow conditions.

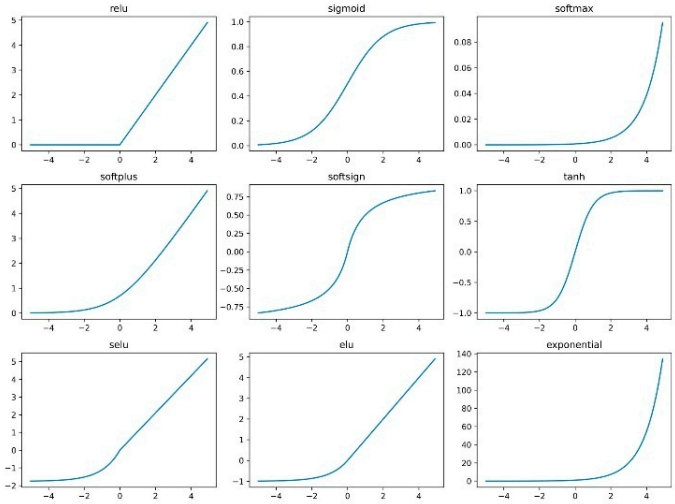


Figure 8. Activation functions.

3.4.1. ESP High-Viscosity Flow

This section analyzes the impact of different activation functions on the prediction of ESP performance under high-viscosity flow conditions. A comparison of Figures 9 and 10 highlights the significant influence of the training dataset on the FNN models. However, due to the inherent limitations of experimental testing, engineers often face two options: manually creating additional "synthetic" data points to control the FNN fitting shape—similar to polynomial fitting—or carefully developing appropriate FNN model structures.

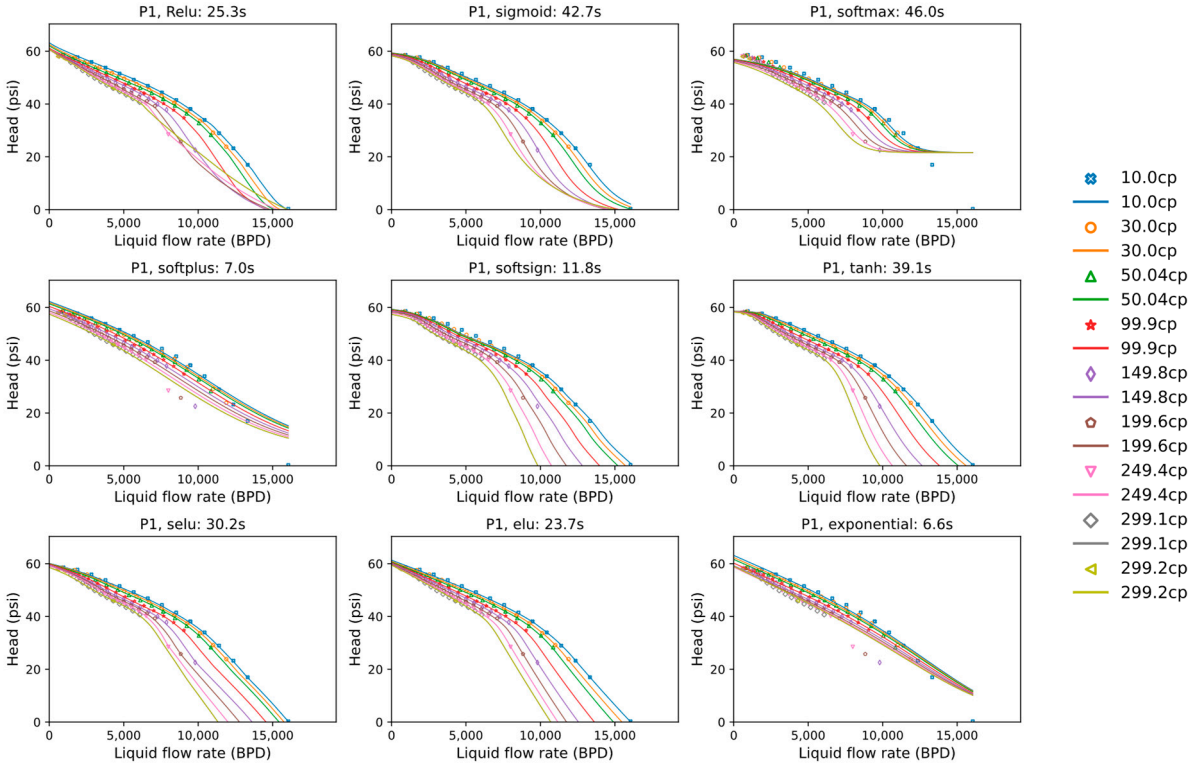


Figure 9. ESP3 high-viscosity performance predictions.

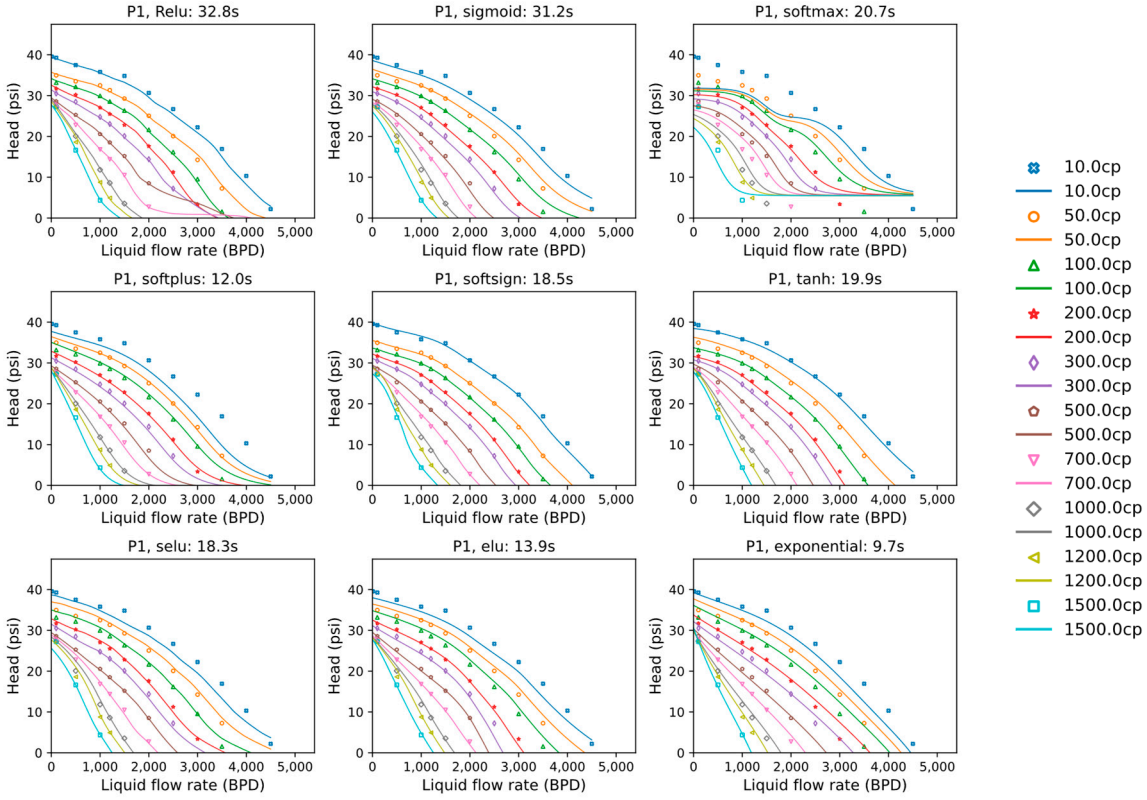


Figure 10. MTESP high-viscosity performance predictions.

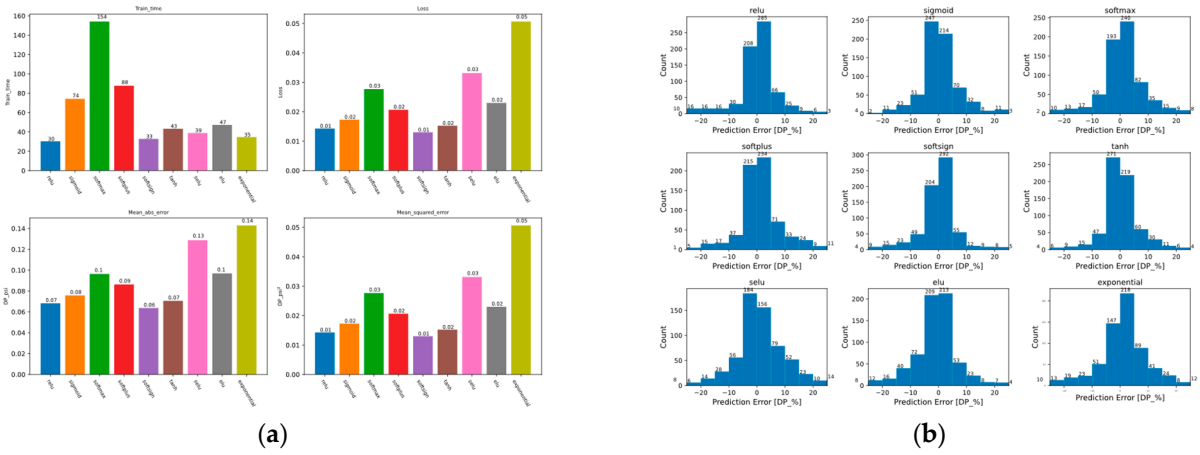
While automated frameworks simplify the process of building FNN structures, reducing the tuning parameter range can substantially lower the computational costs and enhance the prediction accuracy. For instance, as shown in Figure 8, activation functions such as softsign, tanh, selu and elu are recommended for high-viscosity ESP performance

curves because their predictions align closely with the general shape of the pump performance curve.

In Figure 10, the FNN model, using the exact same structure and activation functions as in Figure 9, was trained on another dataset: the high-viscosity curve dataset from the MTESP pump. This dataset was generated through CFD simulations, which were first validated against experimental results and then extended to include data points for the high-flow-rate and high-viscosity conditions. Despite the FNN model structure not being finely tuned for this dataset, the predictions remained highly accurate. Notably, only the FNN models with the softsign, tanh, and elu activation functions successfully predicted pump curves that closely aligned with the physical curve shape. Given the comparable results between Figures 9 and 10, it is evident that the choice of activation function plays a significant role in the accurate prediction of ESP pump curves. The softsign, tanh, and elu activation functions are highly recommended for such tasks. Alternatively, the selu and exponential functions may also be used as substitutes if required.

3.4.2. ESP Gas–Liquid Flow

Figure 11 presents an error heatmap alongside training performance metrics, including the convergence time, loss, mean absolute error (MAE), and mean squared error (MSE), which were used to evaluate the accuracy of each activation function. Among the models, the FNNs with the softsign, relu, and tanh activation functions ranked as the top three performers in predicting the ESP gas–liquid performance. These models achieved relatively faster training times while maintaining lower losses.



(**a**) (**b**)

Figure 11. Error analysis of different activation functions in ESP gas–liquid flow. (**a**) Training time and error analysis. (**b**) Error distribution.

As shown in Figure 12, the FNNs with the softsign, relu, and tanh activation functions produced smoother and more realistic performance curves across the gas–liquid flow conditions. However, in Figure 13, they show slight discrepancies in the surging region, where the softmax function outperforms the others. It is worth noting that the sigmoid and exponential functions exhibited smoother behavior; however, their relatively higher error makes it an engineering decision to balance the trade-off between accuracy and the desired shape of the predicted pump curves.

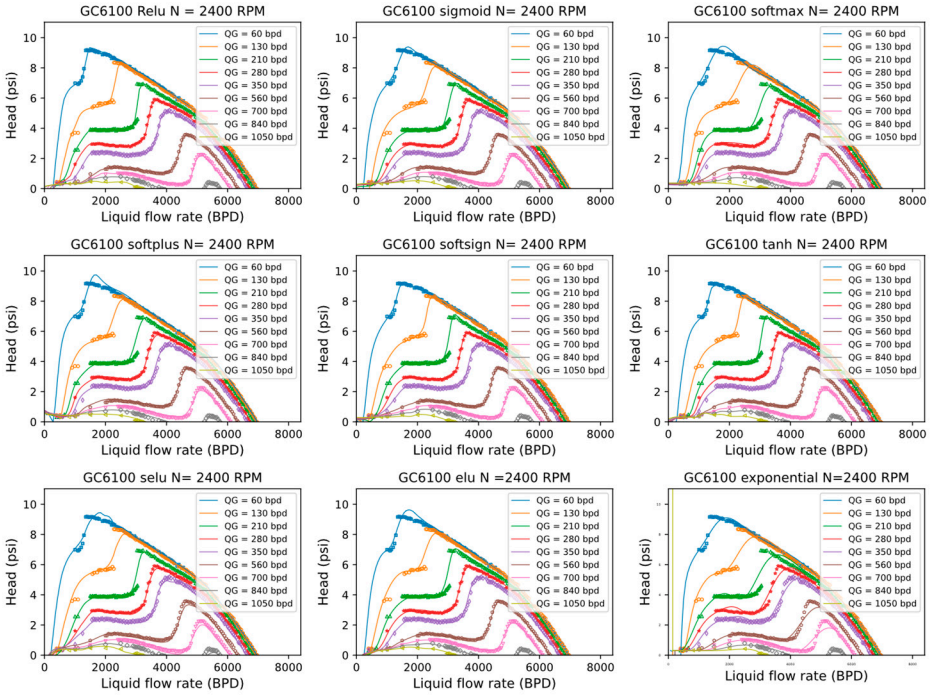


Figure 12. GC6100 gas–liquid flow at 2400 RPM by NN model with different activation functions.

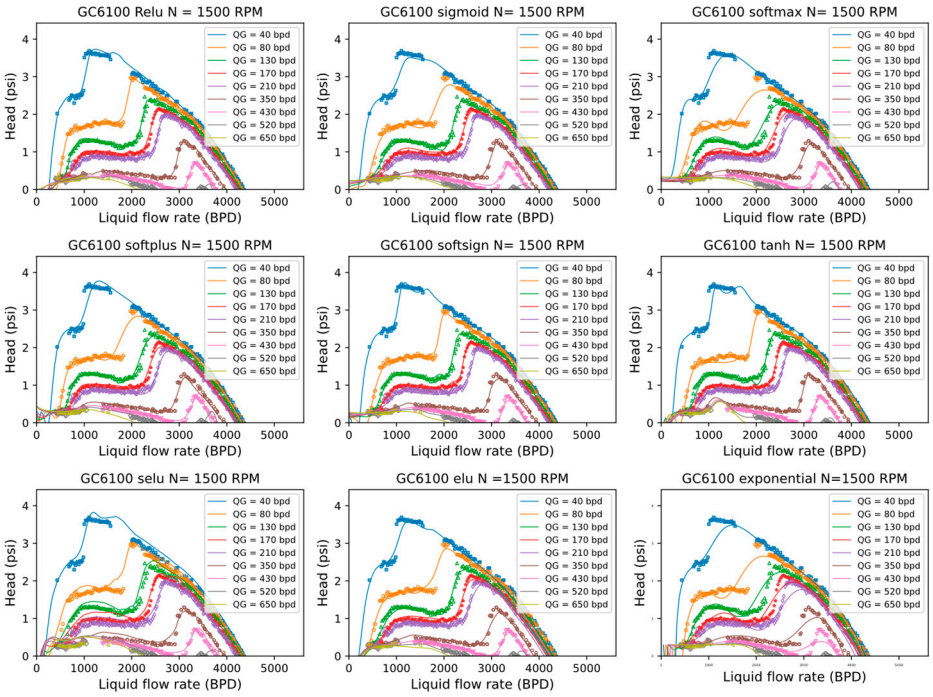


Figure 13. GC6100 gas–liquid flow at 1500 RPM by NN model with different activation functions.

3.5. Training Size Sensitivity and Implications for Future ESP Testing

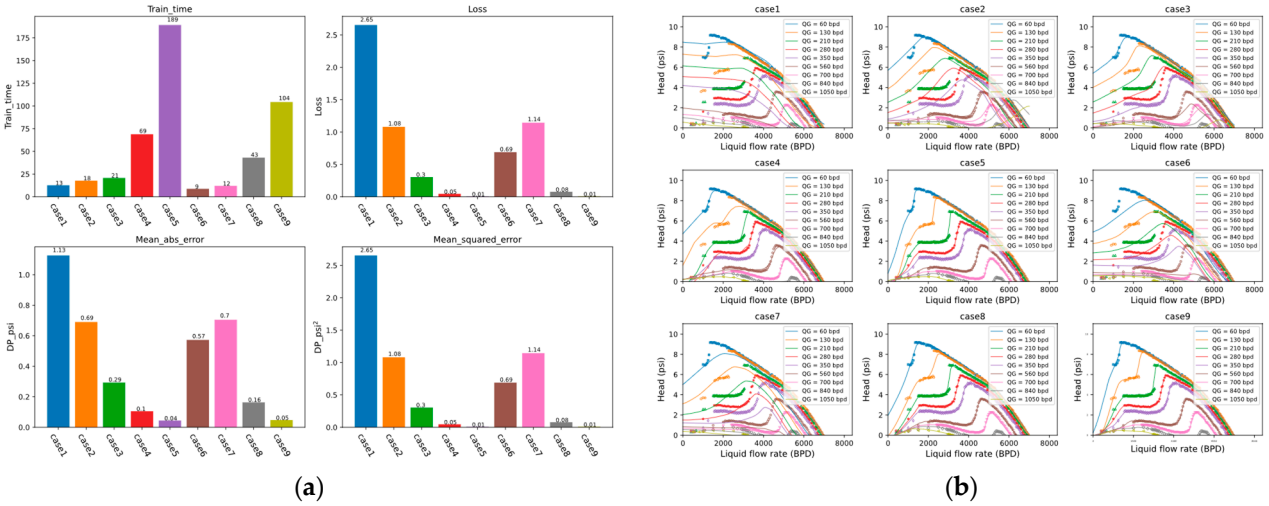
The aim of this section was to determine whether the number of tested pump curves could be reduced while still retaining the model's predictive capabilities. Nine different test matrices of the ESP gas–liquid surging test, i.e., keeping the gas flow rate the same while changing the liquid flow rate, were investigated. In Table 3, Case 1–5 study the gas flow rate effect and Case 6–9 study the rotational speed effect. Case 5 and Case 9 represent a complete ESP gas–liquid surging test, consisting of 36 pump curves, which is a time-consuming and costly process. The goal was to determine the minimum number

of pump curve tests required to maintain the accuracy of the neural network (NN) model, thereby minimizing the time and cost.

Table 3. Effect of testing size and composition on NN model accuracy.

Case	RPM	Gas Flow Rate
1	1500, 1800, 2400, 3000	60, 1050
2	1500, 1800, 2400, 3000	60, 560, 1050
3	1500, 1800, 2400, 3000	60, 350, 700, 1050
4	1500, 1800, 2400, 3000	60, 310, 350, 500, 1050
5	1500, 1800, 2400, 3000	60, 130, 210, 280, 350, 560, 700, 840, 1050
6	1500, 3000	60, 130, 210, 280, 350, 560, 700, 840, 1050
7	1800, 3000	60, 130, 210, 280, 350, 560, 700, 840, 1050
8	1500, 1800, 3000	60, 130, 210, 280, 350, 560, 700, 840, 1050
9	1500, 1800, 2400, 3000	60, 130, 210, 280, 350, 560, 700, 840, 1050

The optimal FNN model structure for each case was determined using the Optuna framework. Figures 14 and 15 demonstrate that incorporating the calculated GVF parameter significantly improved the modeling accuracy, particularly in the surging region, despite that fact that the GVF was directly calculated from the measured liquid and gas flow rates. By training the FNN model with the calculated GVF, the predicted ESP gas–liquid pump curve showed remarkable agreement in both its shape and value, validating that a properly tuned FNN model can effectively capture the underlying fluid flow mechanisms in complex two-phase pump flow behavior. Consequently, this approach offers the potential to reduce the pump testing matrix, thereby lowering costs in future pump testing endeavors.

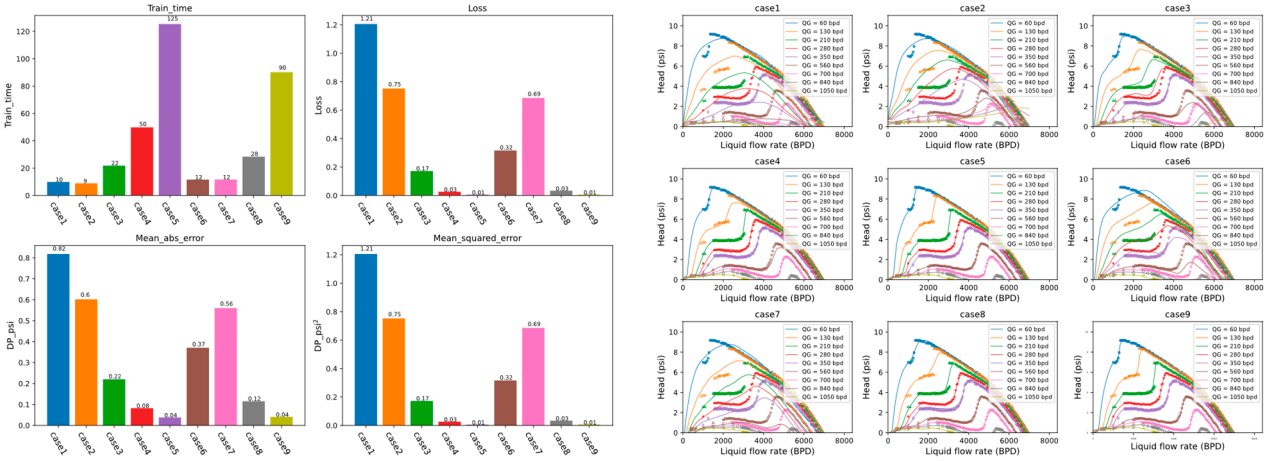


(**a**) (**b**)

Figure 14. FNN model result for different testing case examples (inputs: Ql, Qg, RPM). (**a**) Training time and error analysis. (**b**) Error distribution.

The complete dataset (Cases 5 and 9) exhibited the highest accuracy, as expected, with the smallest errors in both the MSE and the MAE. However, achieving these required significant resources to complete all the tests, rendering it impractical for many applications. Case 1, which had the least training data for the gas flow rates, showed the highest mean squared error (MSE) and mean absolute error (MAE), as evident from the error and performance prediction plots. This underscores the importance of sufficient data coverage, particularly for gas flow rates, to ensure better generalization and reduce deviations from the true values. Increasing the granularity of the gas flow rate data (as seen from Cases 1 to 5) generally improved the prediction accuracy, although diminishing returns were observed beyond a

certain level of granularity. In the speed effect cases (6–9), predictions at 2400 RPM—only included in Case 9's training dataset—revealed high errors in Cases 6 and 7. This suggests that the FNN model did not adequately align with the centrifugal pump affinity law, which describes the proportional relationship between flow, head, and horsepower adjustments.



(**a**) (**b**)

Figure 15. FNN model result for different testing case examples (inputs: Ql, Qg, RPM, GVF). (**a**) GC6100 gas–liquid flow mechanistic model result. (**b**) GC6100 gas–liquid flow mechanistic model error.

For future testing, the findings suggest adopting a selective approach by optimizing the set of gas flow rates to balance the cost, time, and model accuracy. This streamlined approach would support a more efficient testing process while maintaining robust neural network model predictions. It is likely that using three rotational speeds and 4–5 gas flow rates would represent the minimum requirement for achieving this balance. Prioritizing a broader range of gas flow rates over additional speed tests is strongly recommended.

4. Conclusions

This study evaluates the application of different machine learning methods to predict Electric Submersible Pump (ESP) performance under high-viscosity flow and gas–liquid flow conditions. The results indicate that the FNN model outperformed the other six machine learning methods, as well as traditional methods like polynomial fitting and mechanistic modeling, offering improved accuracy, adaptability, and cost-efficiency, even with limited training data. This study also addressed key factors such as overtraining, activation function selection, and dataset size optimization, demonstrating the potential of FNNs as a robust alternative for ESP performance prediction. Detailed conclusions are summarized below:

1. Traditional polynomial fitting methods have the most constraints and are challenging to tune for accurately predicting ESP gas–liquid flow performance. While mechanistic models do not require testing, their applicability is limited by specific conditions and the need for complex input parameters.
2. The FNN model outperforms all the other machine learning methods in both ESP high-viscosity flow and gas–liquid flow. On the other hand, the GPR model can still be used for a relatively smaller dataset (e.g., 1000 data points), and the KRR model can be used but needs to be carefully tuned to avoid tail-up shaped pump curves.
3. AutoML frameworks, like Optuna, streamline optimization but are computationally intensive and require careful application to ensure physical interpretability. Narrow-

ing the parameter ranges and optimizing the activation functions (e.g., softsign and Tanh) significantly enhance the FNN's performance and reduce computational costs.

4. Although the GVF is directly calculated by measuring the liquid and gas flow rate, it significantly improves the FNN model prediction in ESP gas–liquid flow. Future studies could be focused on including more calculated or dimensionless parameters to improve the training speed and reliability.
5. The use of FNN models significantly reduces the need for tested pump curves compared to traditional polynomial fitting methods. For each fluid property, it is recommended to conduct five pump curve tests at three different speeds.
6. The FNN model demonstrates adaptability and physical consistency, even with sparse data. Future research should focus on developing universal neural network models that incorporate time-dependent variables and can generalize across diverse ESP configurations and flow conditions.

In conclusion, the FNN provides a promising alternative to traditional ESP performance prediction methods, offering enhanced adaptability, accuracy, and cost-efficiency. Future work should focus on expanding the training dataset to include more complex scenarios and further refining the network to optimize its predictive capabilities across a broader range of operating conditions.

Author Contributions: Conceptualization, H.Z. and H.Y.; methodology, H.Z.; software, Q.S.; validation, H.Z., H.Y. and Q.S.; formal analysis, H.Z.; investigation, Q.W. and H.J.; resources, H.Y.; data curation, R.A.; writing—original draft preparation, H.Z.; writing—review and editing, H.Y.; visualization, H.J.; supervision, H.Z.; project administration, H.Z.; funding acquisition, H.Z. All authors have read and agreed to the published version of the manuscript.

Funding: This research received no external funding.

Data Availability Statement: The data supporting the reported results are confidential and accessible only to TUALP member companies. However, the published data related to this study are available in our previous papers.

Acknowledgments: The authors appreciate the TUALP member companies for providing ESPs and research resources.

Conflicts of Interest: The authors declare no conflicts of interest.

References

1. Zhu, H.; Zhu, J.; Zhang, H.Q. Mechanistic modeling of gas effect on Multi-stage Electrical submersible pump (ESP) performance with experimental validation. *Chem. Eng. Sci.* **2022**, *252*, 117288. [CrossRef]
2. Deng, X.; Yuan, S.; Si, Q.; Li, Y.; Pei, J.; Yuan, J. Seismic response analysis of residual heat removal pump considering transient fluid excitation force in 1000-MW nuclear power plants. *J. Vibroeng.* **2014**, *16*, 965–976.
3. Deng, X. A mixed zero-equation and one-equation turbulence model in fluid-film thrust bearings. *J. Tribol.* **2024**, *146*, 034101. [CrossRef]
4. Wang, Q.; Huang, Q.; Sun, X.; Zhang, J.; Karimi, S.; Shirazi, S.A. Experimental and numerical evaluation of the effect of particle size on slurry erosion prediction. *J. Energy Resour. Technol.* **2021**, *143*, 073101. [CrossRef]
5. Wang, Q.; Huang, Q.; Wang, N.; Wen, Y.; Ba, X.; Sun, X.; Zhang, J.; Karimi, S.; Shirazi, S.A. An experimental and numerical study of slurry erosion behavior in a horizontal elbow and elbows in series. *Eng. Fail. Anal.* **2021**, *130*, 105779. [CrossRef]
6. Van Rensburg, N.J. Guest Editorial: Artificial Intelligence Can Reduce ESP Failures. *J. Pet. Technol.* **2019**, *71*, 16–17. [CrossRef]
7. Alamu, O.A.; Pandya, D.A.; Warner, O.; Debacker, I. ESP data analytics: Use of deep autoencoders for intelligent surveillance of electric submersible pumps. In Proceedings of the Offshore Technology Conference, Houston, TX, USA, 4–7 May 2020; p. D011S013R006.
8. Melo, R.A.; Worth, D.J.; Swaffield, S. Assessment of Real-Time ESP Failure Prediction Using Digital Twin, Machine Learning and Damage Modelling. In Proceedings of the SPE Gulf Coast Section-Electric Submersible Pumps Symposium, The Woodlands, TX, USA, 2–6 October 2023.

9. Pham, S.T.; Vo, P.S.; Nguyen, D.N. Effective Electrical submersible pump management using machine learning. *Open J. Civ. Eng.* **2021**, *11*, 70–80. [CrossRef]
10. Alrowayyeh, J.; Dhote, P.; Alqenaei, A. Machine Learning Model for Efficient Surveillance of Electrostatic Pump Operations & Predictive Analytics for Early Alarming System. In Proceedings of the SPE Conference at Oman Petroleum & Energy Show, Muscat, Oman, 22–24 April 2024; p. D031S032R004.
11. Han, W.; Nan, L.; Su, M.; Chen, Y.; Li, R.; Zhang, X. Research on the prediction method of centrifugal pump performance based on a double hidden layer BP neural network. *Energies* **2019**, *12*, 2709. [CrossRef]
12. Dutta, N.; Umashankar, S.; Shankar, V.A.; Padmanaban, S.; Leonowicz, Z.; Wheeler, P. Centrifugal pump cavitation detection using machine learning algorithm technique. In Proceedings of the 2018 IEEE International Conference on Environment and Electrical Engineering and 2018 IEEE Industrial and Commercial Power Systems Europe (EEEIC/I&CPS Europe), Palermo, Italy, 12–15 June 2018; pp. 1–6.
13. Mohammadzaheri, M.; Tafreshi, R.; Khan, Z.; Ghodsi, M.; Franchek, M.; Grigoriadis, K. Modelling of petroleum multiphase flow in electrical submersible pumps with shallow artificial neural networks. *Ships Offshore Struct.* **2020**, *15*, 174–183. [CrossRef]
14. Mohammadzaheri, M.; Tafreshi, R.; Khan, Z.; Franchek, M.; Grigoriadis, K. An intelligent approach to optimize multiphase subsea oil fields lifted by electrical submersible pumps. *J. Comput. Sci.* **2016**, *15*, 50–59. [CrossRef]
15. Syed, F.I.; Alshamsi, M.; Dahaghi, A.K.; Neghabhan, S. Artificial lift system optimization using machine learning applications. *Petroleum* **2022**, *8*, 219–226. [CrossRef]
16. Kumar, A.; Gandhi, C.P.; Zhou, Y.; Kumar, R.; Xiang, J. Improved deep convolution neural network (CNN) for the identification of defects in the centrifugal pump using acoustic images. *Appl. Acoust.* **2020**, *167*, 107399. [CrossRef]
17. Orrù, P.F.; Zoccheddu, A.; Sassu, L.; Mattia, C.; Cozza, R.; Arena, S. Machine learning approach using MLP and SVM algorithms for the fault prediction of a centrifugal pump in the oil and gas industry. *Sustainability* **2020**, *12*, 4776. [CrossRef]
18. Guo, D.; Raghavendra, C.S.; Yao, K.T.; Harding, M.; Anvar, A.; Patel, A. Data driven approach to failure prediction for electrical submersible pump systems. In Proceedings of the SPE Western Regional Meeting, Garden Grove, CA, USA, 27–30 April 2015; p. SPE-174062.
19. Zhu, J.; Zhu, H.; Cao, G.; Zhang, J.; Peng, J.; Banjar, H.; Zhang, H.Q. A new mechanistic model to predict boosting pressure of electrical submersible pumps under high-viscosity fluid flow with validations by experimental data. *SPE J.* **2020**, *25*, 744–758. [CrossRef]
20. Barrios, L.; Prado, M.G. Experimental visualization of two-phase flow inside an electrical submersible pump stage. *J. Energy Resour. Technol.* **2011**, *133*, 042901. [CrossRef]
21. Zhu, J.; Banjar, H.; Xia, Z.; Zhang, H.Q. CFD simulation and experimental study of oil viscosity effect on multi-stage electrical submersible pump (ESP) performance. *J. Pet. Sci. Eng.* **2016**, *146*, 735–745. [CrossRef]
22. Wood, S.N. *Generalized Additive Models: An Introduction With R*; Chapman and Hall/CRC: New York, NY, USA, 2017.
23. Smola, A.J.; Schölkopf, B. A tutorial on support vector regression. *Stat. Comput.* **2004**, *14*, 199–222. [CrossRef]
24. Williams, C.K.; Rasmussen, C.E. *Gaussian Processes for Machine Learning*; MIT Press: Cambridge, MA, USA, 2006; Volume 2, p. 4.
25. Zhao, H. Neural network with data augmentation in multi-objective prediction of multi-stage pump. *arXiv* **2020**, arXiv:2002.02402.
26. Chen, T.; Guestrin, C. August. Xgboost: A scalable tree boosting system. In Proceedings of the 22nd ACM SIGKDD International Conference on Knowledge Discovery and Data Mining, San Francisco, CA, USA, 13–17 August 2016; pp. 785–794.
27. Saunders, C.; Gammerman, A.; Vovk, V. Ridge regression learning algorithm in dual variables. In Proceedings of the 15th International Conference on Machine Learning, Madison, WI, USA, 24–27 July 1998.

Disclaimer/Publisher's Note: The statements, opinions and data contained in all publications are solely those of the individual author(s) and contributor(s) and not of MDPI and/or the editor(s). MDPI and/or the editor(s) disclaim responsibility for any injury to people or property resulting from any ideas, methods, instructions or products referred to in the content.